



**WITHHOLD ENCLOSURE 3 FROM PUBLIC DISCLOSURE  
UNDER 10 CFR 2.390 and 9.17**

August 12, 2009

L-MT-09-043  
10 CFR 50.90

U. S. Nuclear Regulatory Commission  
ATTN: Document Control Desk  
Washington, DC 20555-0001

Monticello Nuclear Generating Plant  
Docket 50-263  
Renewed Facility Operating License  
License No. DPR-22

Monticello Extended Power Uprate: Response to NRC Mechanical and Civil Engineering Review Branch (EMCB) Requests for Additional Information (RAIs) dated March 20, 2009, and June 26, 2009 (TAC No. MD9990)

- References:
1. NSPM letter to NRC, License Amendment Request: Extended Power Uprate (L-MT-08-052) dated November 5, 2008, Accession No. ML083230111
  2. Email P. Tam (NRC) to G. Salamon, K. Pointer (NSPM) dated March 20, 2009, "Monticello - Draft RAIs from Mechanical & Civil engineering Branch re: proposed EPU amendment (TAC MD9990)" Accession No. ML090820015
  3. Email P. Tam (NRC) to G. Salamon, L. Gunderson, K. Pointer (NSPM) dated June 26, 2009, "Monticello - Proposed EPU Amendment, additional draft question re: steam dryer (TAC MD9990)" Accession No. ML091800009

Pursuant to 10 CFR 50.90, the Northern States Power Company, a Minnesota corporation (NSPM), requested in Reference 1 an amendment to the Monticello Nuclear Generating Plant (MNGP) Renewed Operating License (OL) and Technical Specifications to increase the maximum authorized power level from 1775 megawatts thermal (MWt) to 2004 MWt.

On March 20, 2009, the U.S. Nuclear Regulatory Commission (NRC) Mechanical and Civil Engineering Review Branch (EMCB) provided the requests for additional information (RAI) contained in Reference 2. On June 26, EMCB provided an additional RAI contained in Reference 3. Enclosure 1 provides the non proprietary response to EMCB RAIs in References 2 and 3. A portion of NSPM's response to EMCB RAIs contains information considered proprietary to Continuum Dynamics Incorporated (CDI). A proprietary version of Enclosure 1 is contained in Enclosure 3. CDI requests this proprietary information to be

withheld from public disclosure in accordance with 10 CFR 2.390(a)4 and 9.17(a)4. An affidavit supporting this request is provided in Enclosure 2.

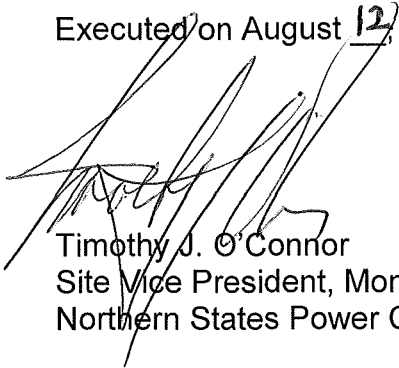
In accordance with 10 CFR 50.91, a copy of this letter is being provided to the designated Minnesota Official without the proprietary version.

Summary of Commitments

1. NSPM will provide the evaluation of steam dryer structural integrity to the NRC staff prior to further increases in reactor power when increasing to power levels above CLTP.
2. NSPM will perform outage steam dryer inspections based on the guidance of BWRVIP.

I declare under penalty of perjury that the foregoing is true and correct.

Executed on August 12, 2009.



Timothy J. O'Connor  
Site Vice President, Monticello Nuclear Generating Plant  
Northern States Power Company - Minnesota

Enclosures

cc: Administrator, Region III, USNRC  
Project Manager, Monticello, USNRC  
Resident Inspector, Monticello, USNRC  
Minnesota Department of Commerce

**ENCLOSURE 1**

**NSPM RESPONSE TO EMCB RAIs DATED MARCH 20, 2009 and JUNE 26, 2009**

**(Non Proprietary)**

### EMCB-SD RAI No. 1

The executive Summary of CDI Report 07-25P states that the dryer pressure loading at CLTP conditions was computed using the methodology in BWRVIP-194, "BWR Vessel and Internals Project, Methodologies for Demonstrating Steam Dryer Integrity for Power Uprate" with the exception that the EIC signal was not used. However, BWRVIP-194 has not been reviewed and accepted by the staff. References to documents that were not reviewed and accepted by the staff are not acceptable. The licensee is requested to replace reference to BWRVIP-194 by a stand alone document that contains all applicable technical information that supports the structural adequacy of the reactor internals under uprated power conditions.

### NSPM Response

Technical areas referenced to BWRVIP-194 are addressed in RAI 5, 6, 7, 8, 9, 10, 11, and 12. Rather than a single stand-alone document written to support NSPM responses to these RAIs, NSPM will include the applicable technical discussion in each specific RAI response, and remove all references to BWRVIP-194.

### EMCB-SD RAI No. 2

- (a) CDI Report 07-25P states that the signals due to pipe vibration have been removed from the MSL data at frequencies between 14 and 34 Hz.
- i. Provide details on how and why these signals were removed.
  - ii. At which frequencies were signals removed? How much (percentage) of the signals were removed?
  - iii. How were the peaks at these frequencies positively identified as vibrations due to pipe bending?
- (b) Did any of the MSL strain gages fail during CLTP or Low Power (LP) data acquisition? If so, provide details on the number of strain gage failures and the cause for such failures?

### NSPM Response

[[

(3)]

[[

(3)]

Strain gage installation and monitoring were undertaken by Structural Integrity and reported in SI Report No. SIS-07-001, "Monticello EPU Main Steam Dynamic Pressure Monitoring Data Acquisition Specification," wherein it is shown that eight strain gages were located around the circumference of each main steam line at two locations per line. Figure 2.1 illustrates the positions of the strain gages. Strain gage data were reported in pairs, for example A01/A05, A02/A06, etc. For the purpose of illustration, NSPM plotted the PSDs of the raw data signals for each pair, converted to pressures, for main steam lines A and B, in Figures 2.2 and 2.3. No filtering was done to these data for these plots. The original data, recorded as a function of time, were provided by SI in the file identified as 20070613105949 for CLTP conditions.

As it may be seen, strain gage pairs do not give the same pressure signal. Pipe thickness measurements and the misalignment of strain gages may be partly responsible for this effect.

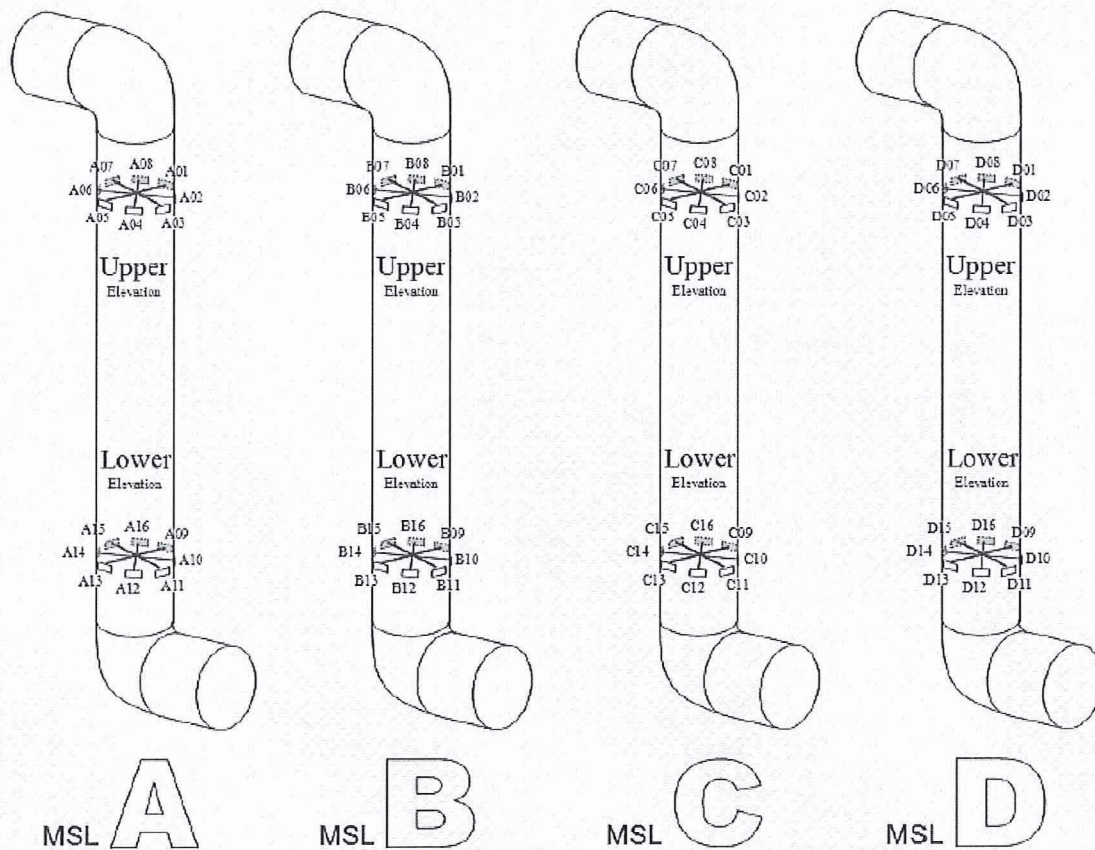


Figure 2.1: Monticello Strain Gage Layout

[[

<sup>(3)</sup>]]

Figure 2.2: Pressure PSDs of strain gage pairs on main steam line A at CLTP conditions: upper location (top); lower location (bottom). See Figure 2.1 for strain gage locations.

[[

<sup>(3)</sup>]]

Figure 2.3: Pressure PSDs of strain gage pairs on main steam line B for CLTP conditions: upper location (top); lower location (bottom). See Figure 2.1 for strain gage locations.



(b) NSPM has had a trend in failures at Monticello, where it found 38 of the original 64 failed. While evaluations to date have been inconclusive, the investigation continues. A current theory is that the AC induced currents and voltages occur in the penetration due to the 480 VAC power going through the same penetration leads to a fatigue failure of the strain gages. NSPM replaced 19 gages during the Spring 2009 outage and will open the circuit when not taking data, in an attempt to resolve failures. This procedure should provide a larger number of gages available during power ascension.

The 2007 CLTP data had a full set of gages except for the low power data where main steam line C did not have data due to DAS issues (not strain gage failures). Low power data were collected during Fall 2008 with the 480 VAC power turned off. This data set had signals with significantly reduced electrical noise content and was used to evaluate the steam dryer along with the 2007 CLTP data.

Based on the number of replaced gages and the open circuit configuration while the system is not in use, there should be sufficient functioning gages to perform the evaluation to the limit curves. Prior to the collection of the data for evaluation purpose NSPM will perform a test to verify that sufficient gages are available.

### EMCB-SD RAI No. 3

Clarify the statement on Page 5 of CDI Report 07-25P: "...and the phasing of the replaced data on main steam line C was varied until the minimum peak PSD on the dryer ... was determined." How did NSPM determine that minimizing the peak PSD at one point on the dryer at low power conditions would lead to conservative MSL spectra at CLTP conditions following noise removal?

### NSPM Response

The approach described in the RAI was used to substitute for missing 2007 low power data, because of strain gage failure on MSL C. An explanation of this approach is no longer relevant, as NSPM has substituted the 2008 low power data for the 2007 low power data (per the suggestion in RAI 5). The 2008 data set was complete.

EMCB-SD RAI No. 4

Provide contour plots and a discussion on the source of the dryer loads at frequencies near 99 Hz, where a strong peak appears in the loading PSDs in Figure 4.6 of CDI Report 07-25P.

NSPM Response

[[

(3)]]

L-MT-09-043  
Enclosure 1  
Non Proprietary  
Page 8 of 64

[[

(3)]]

[[

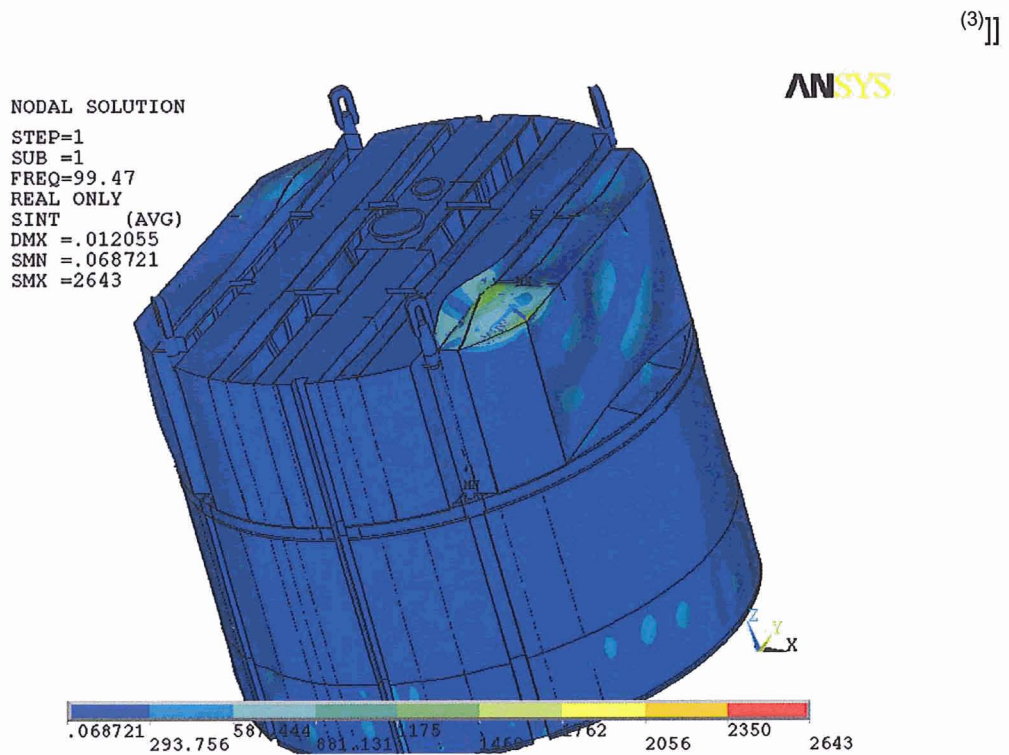


Figure 4.3: Pressure contour plot produced by a unit pressure imposed at main steam line A at 99.47 Hz (top) and corresponding stress intensity (bottom).

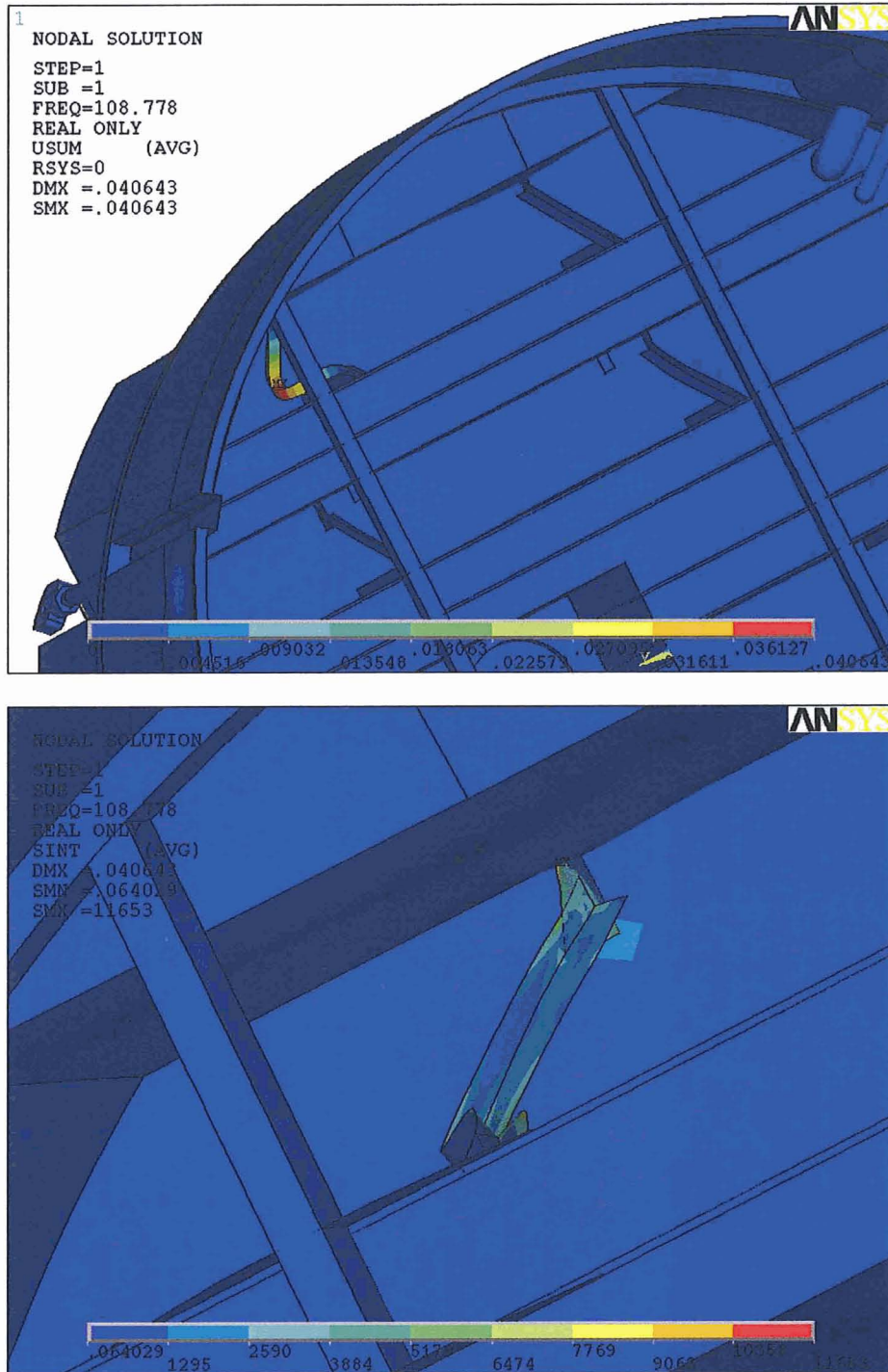


Figure 4.4: Displacement contours (top) and stress contours (bottom) resulting from a unit pressure over the main steam line A inlet at 108.8 Hz.

### EMCB-SD RAI No. 5

CDI Report 07-25P discusses noise removal from the CLTP signal. The licensee is advised to note the staff's position that using noise removal from CLTP signals based on LP signals is only acceptable when the LP signals are not corrupted by background electrical interference (EIC) noise, otherwise the dryer stresses should be computed using original CLTP signals, not those reduced by the LP signals corrupted by EIC noise. The licensee is requested to provide a discussion of the LP noise that was subtracted from CLTP and clearly substantiates that the LP signal is affected or corrupted by EIC. NSPM may submit new data and stress analyses based on low power signals not corrupted by EIC noise, for the staff's consideration.

### NSPM Response

The original CLTP and low power data were collected in May and April of 2007. At that time Monticello did not record EIC data. Low power and EIC data were subsequently collected in September and October 2008; however, the EIC data at CLTP conditions was judged unusable because of the large frequency exclusion that would be required at 60 Hz. Thus, in all analyses discussed, the 2007 CLTP did NOT have the 2008 CLTP EIC data removed, whereas for a conservative result, the 2008 Low Power data did have the 2008 Low Power EIC data removed. Figures 5.1 to 5.4 plot the CLTP (EIC not removed) and low power data (EIC removed). Note that the low power signals are consistently lower at each strain gage location than the CLTP signals for the frequency range considered here.

Comparisons between EIC and low power data (with EIC included) are shown in Figures 5.5 to 5.8. It may be seen that the low power data are consistently higher than the EIC data, except at the exclusion frequencies (60, 120, 180 Hz) where the two signals (at each strain gage location) are essentially the same.

Further comparisons, between the CLTP data collected in 2007 and the CLTP data collected in 2008 (again, with EIC not removed), are shown in Figures 5.9 to 5.12. Both sets of signals are comparable, [[

<sup>(3)</sup>]] For this reason the 2007 data were used for the Monticello dryer analysis.

[[

Figure 5.1: Pressure PSDs on main steam line A for the 2007 CLTP data (EIC not removed) and 2008 Low Power data (EIC removed).<sup>(3)</sup>]]

[[

Figure 5.2: Pressure PSDs on main steam line B for the 2007 CLTP data (EIC not removed) and 2008 Low Power data (EIC removed).<sup>(3)</sup>]]



[[

Figure 5.3: Pressure PSDs on main steam line C for the 2007 CLTP data (EIC not removed) and 2008 Low Power data (EIC removed).

<sup>(3)</sup>]]

[[

Figure 5.4: Pressure PSDs on main steam line D for the 2007 CLTP data (EIC not removed) and 2008 Low Power data (EIC removed).

<sup>(3)</sup>]]

[[

Figure 5.5: Pressure PSDs on main steam line A for the 2008 Low Power data with EIC<sup>(3)</sup> included and the 2008 EIC data taken at low power conditions. ]]

[[

Figure 5.6: Pressure PSDs on main steam line B for the 2008 Low Power data with EIC included and the 2008 EIC data taken at low power conditions. <sup>(3)</sup>]]

[[

Figure 5.7: Pressure PSDs on main steam line C for the 2008 Low Power data with EIC<sup>(3)</sup> included and the 2008 EIC data taken at low power conditions.

[[

Figure 5.8: Pressure PSDs on main steam line D for the 2008 Low Power data with EIC<sup>(3)</sup> included and the 2008 EIC data taken at low power conditions.]]

[[

Figure 5.9: Pressure PSDs on main steam line A for the 2007 CLTP data (EIC not removed) and 2008 CLTP data (EIC not removed).<sup>(3)</sup>]]

[[

Figure 5.10: Pressure PSDs on main steam line B for the 2007 CLTP data (EIC not removed) and 2008 CLTP data (EIC not removed).<sup>(3)</sup>]]



[[

Figure 5.11: Pressure PSDs on main steam line C for the 2007 CLTP data (EIC not removed) and 2008 CLTP data (EIC not removed).<sup>(3)</sup>]]

[[

Figure 5.12: Pressure PSDs on main steam line D for the 2007 CLTP data (EIC not removed) and 2008 CLTP data (EIC not removed).<sup>(3)</sup>]]

### EMCB-SD RAI No. 6

There appears to be an inconsistency among the different NSPM reports regarding how the CLTP signals are reduced by the low power signals. On Page 16 of 24 of Enclosure 11 to L-MT-08-052, "Steam Dryer Dynamic Stress Evaluation", NSPM states that, "For consistency, the low power strain gage signals are filtered in the same manner as the CLTP data and are fed into the ACM model to obtain the monopole and dipole signals at the MSL inlets." In Report CDI 07-25P, "Acoustic and Low Frequency Hydrodynamic Loads at CLTP Power Level on Monticello Steam Dryer to 200 Hz", Rev. 4, November 2008, NSPM states that up to 80% of the low power strain gage signals was subtracted from those measured at CLTP. In a third report, CDI Report 07-26P, "Stress Assessment of Monticello Steam Dryer", Rev. 2, November 2008, Equation 8 indicates that the CLTP signal is reduced by up to 80% (not that up to 80% of the LF signal is subtracted from the CLTP signals). Clearly, the wording in these three reports is contradictory. NSPM is requested to resolve the discrepancies and explain clearly how the low power noise removal was implemented. In addition, NSPM is requested to modify the above mentioned reports so that the procedure of low power noise removal is consistent among the three reports.

### NSPM Response

The equation, as defined in C.D.I. Report No. 07-25P (the loads report) and C.D.I. Report No. 07-26P (the stress report), is

$$P_R(\omega) = P_S(\omega) \left[ 1 - \left| \frac{P_L(\omega)}{P_S(\omega)} \right| \right]$$

where  $P_R(\omega)$  is the CLTP signal  $P_S(\omega)$  corrected for Low Power  $P_L(\omega)$ , computed as a function of frequency  $\omega$ , and  $|P_L(\omega)/P_S(\omega)|$  can be no larger than 0.8. This factor suggests that the CLTP signal is reduced by no more than 80% of the original signal. This interpretation is consistent with the wording in both C.D.I. reports. Page 16 of 24 of Enclosure 11 to L-MT-08-052 (supplied by NSPM) is in error.

See also the response to EMCB-SD- RAI 20, where it is shown that noise subtraction is not required for stress ratios above 2.0 at EPU conditions.

EMCB-SD RAI No. 7

The proper filtering of the plant noise (low power signal) from the CLTP signal requires that the corresponding EIC signals are accounted for. That is, the low power and CLTP signals are modified by subtracting the corresponding EIC signals from them, and then the modified LP signal is filtered out from the modified CLTP signal. Such a procedure was considered acceptable during staff's review of previous EPU application that CDI was involved in. However for the Monticello steam dryer, as stated in CDI Report 07-25P, NSPM has decided not to modify the LP and CLTP signals by subtracting the corresponding EIC signals. The licensee is requested to justify that this approach of not using the EIC signal is conservative compared to the one used for the BFN Unit 1 steam dryer.

NSPM Response

The 2008 low power and EIC data sets have been used with the 2007 CLTP data. EIC data are removed from the 2008 low power data (the low power EIC data), but not from the 2007 CLTP data (the CLTP EIC data). The result is conservative.

Previously, when noise subtraction was performed, EIC was left in the CLTP signal but subtracted from low power. This approach produced a conservative signal after noise subtraction, since the low power signal magnitude after EIC subtraction is everywhere less than or equal to the low power signal without EIC subtraction. Hence, a smaller amplitude low power signal was subtracted from the CLTP signal.

Note that currently no low power subtraction is performed, so this issue is not relevant to the current stress analysis.

EMCB-SD RAI No. 8

[[

(3)]]

NSPM Response

[[

(3)]

[[

(3)]

[[

(3)]

[[

[[

(3)]]

(3)]]



EMCB-SD RAI No. 9

[[

(3)]]

NSPM Response

[[

(3)]]

[[

[[

(3)]]

(3)]]

EMCB-SD RAI No. 10

[[

.<sup>(3)</sup>]] The licensee is requested to update the stress results in CDI Report 07-26P to reflect the revised bias errors and uncertainties. Also, the licensee is requested to provide updated limit curves reflecting the revised bias errors and uncertainties indicated in EMCB-SD-RAIs 8, 9, and 10.

NSPM Response

A change in the frequency intervals for bias and uncertainty computation is not justified, based on the stress ratio margin requirements.

[[

<sup>(3)</sup>]]

[[

[[

(3)]]

[[

(3)]]

(3)]]

### EMCB-SD RAI No. 11

The licensee is requested to provide stress ratios at CLTP and EPU conditions based on dryer loads without low power noise removal. These revised stress ratios should take into account EMCB-SD-RAIs 8, 9 and 10 pertaining to (a) reduction of dryer loads at frequencies between 158 and 162 Hz, (b) reduction of the uncertainty associated with the FE model vs. shaker test data, and (c) using revised uncertainties and bias error in the frequency range of 60 to 100 Hz.

### NSPM Response

Responses to RAI 8, 9, and 10 have taken exception to the recalculation requested. However, it is appropriate to provide the stress analysis results for CLTP and EPU conditions without low power noise removal.

Note the following:

1. The locations on the inner and middle vane bank rails where they meet the outer wall of the dryer (previously nodes 21519 and 13858, which were locations 3 and 4 in the list of alternating stress ratios at welds in Table 8b of CDI Report 07-26, Rev. 2) are now processed per the ASME code (Table NG-3352-1) by taking the surrounding nominal stresses and multiplying by a weld quality factor of 4.0. This approach is necessary since these locations are clearly non-convergent, mathematically consistent but physically unrealistic stress singularities. For the engineering purpose of establishing weld integrity it is better to evaluate the associated stress ratio on the basis of local stresses away from the weld and the higher weld factor.
2. In the originally reported values, a stress reduction factor of 0.39 was applied to the weld connecting the outer hood and interior vertical plate. The values reported in the tables herein now use the revised value of 0.85 per the response to RAI 16(i).
3. Results with noise left in do not necessarily agree with the results from CDI Report 07-26, Rev. 2 because of the differences cited above and modifications to the load generation process as described in the response to RAI 2.
4. The results of Table 11.1 for CLTP loads with low power (LP) noise filtering were obtained by performing a complete stress analysis of the entire dryer and identifying the limiting stress locations both with and without frequency shifting. The remaining results for the dryer at EPU (Table 11.2) and CLTP with noise left

in (Table 11.3) were developed using real time analysis applied to the locations in Table 11.1.

Stresses were also re-evaluated for all nodes on a weld having an alternating stress ratio,  $SR_a < 5$  at CLTP with noise filtered. The stresses at these nodes were re-evaluated at various load conditions using the real time analysis which allows inspection of individual nodes. The conditions considered are: (i) CLTP with noise filtered (up to 80% or the original signal can be removed); (ii) CLTP with noise left in (no filtering); (iii) EPU with noise filtered; and (iv) EPU with noise left in. In each case, the limiting alternating stress ratio at any frequency shift is recorded. The results are tabulated in Table 11.5. No credit for any stress reduction factors (SRFs) has been taken in these results.

The overall conclusions from these results are that even without noise filtering or reliance on any stress reduction factors, target alternating stress ratios at both CLTP and EPU are met with considerable margin.

Table 11.1a. Locations with minimum stress ratios for CLTP conditions with no frequency shift. Stress ratios are grouped according to stress type (maximum – SR-P; or alternating – SR-a) and location (away from a weld or at a weld). Bold text indicates minimum stress ratio of any type on the structure. Stress ratios away from welds are all greater than 4.0. Signal noise has been removed from 2007 CLTP signal data using 2008 low power data.

Stress Ratio	Weld	Location	Location (in) <sup>(a)</sup>			node <sup>(b)</sup>	Stress Intensity (psi)			Stress Ratio	
			x	y	z		Pm	Pm+Pb	S <sub>alt</sub>	SR-P	SR-a
SR-P	No	NONE (All SR-P > 4)									
SR-a	No	NONE (All SR-a > 4)									
<b>SR-P</b>	<b>Yes</b>	<b>1. Lifting Rod Support</b>	<b>-50.6</b>	<b>77.8</b>	<b>0</b>	<b>152128</b>	<b>3286</b>	<b>3286</b>	<b>&lt;250</b>	<b>2.83</b>	<b>&gt;20</b>
"	"	2. Inner Top Cover/Rail	-11.1	95.4	61.5	141731	1304	3703	<250	3.76	>20
"	"	3. Middle Plate/Inner Cover Plate (AB)	1.8	0	0	143461	1208	3336	<250	4.18	>20
"	"	4. Inner Vane Bank (CD)	-1.8	-99.7	12	20042	2043	2043	<250	4.55	>20
"	"	5. Inner Cover Plate (CD)	-32.2	91.7	0	112814	583	2905	<250	4.8	>20
SR-a	Yes	1. Outer Hood/Outer Cover Plate (CD)	-84.8	-17	3.6	139060	269	1656	1645	8.42	4.18

Notes for Tables.

- (a) Spatial coordinates are in a reference frame whose origin is located at the intersection of the steam dryer centerline and the plane containing the base plates (this plane also contains the top of the upper support ring and the bottom edges of the hoods). The y-axis is parallel to the hoods, the x-axis is normal to the hoods pointing from MSL C/D to MSL A/B, and the z-axis is vertical, positive up.
- (b) Node numbers are retained for further reference.



Table 11.1b. Locations with minimum stress ratios for CLTP conditions with frequency shifts. Stress ratios at every node are recorded as the lowest stress ratio identified during the frequency shifts. Stress ratios are grouped according to stress type (maximum – SR-P; or alternating – SR-a) and location (away from a weld or at a weld). Bold text indicates minimum stress ratio of any type on the structure. Stress ratios away from welds are all higher than 4.0. Signal noise has been removed from 2007 CLTP signal data using 2008 low power data.

Stress Ratio	Weld	Location	Location (in.) <sup>(a)</sup>			node <sup>(b)</sup>	Stress Intensity (psi)			Stress Ratio		% Freq. Shift
			x	y	z		Pm	Pm+Pb	S <sub>alt</sub>	SR-P	SR-a	
SR-P	No	NONE (All SR-P > 4)										
SR-a	No	NONE (All SR-P > 4)										
<b>SR-P</b>	<b>Yes</b>	<b>1. Lifting Rod Support</b>	<b>-50.6</b>	<b>77.8</b>	<b>0</b>	<b>152128</b>	<b>3433</b>	<b>3433</b>	<b>339</b>	<b>2.71</b>	<b>20.27</b>	<b>10</b>
"	"	2. Inner Top Cover/Rail	-11.1	95.4	61.5	141731	1348	3827	296	3.64	23.2	10
"	"	3. Middle Plate/Inner Cover Plate (AB)	1.8	0	0	143461	1258	3473	256	4.01	26.82	7.5
"	"	4. Inner Vane Bank (AB)	1.8	99.7	12	20737	2167	2167	361	4.29	19.01	10
"	"	5. Middle Vane Bank (AB)	23.2	94.9	12	11016	2139	2139	384	4.35	17.9	10
"	"	6. Top Vane Bank Bar	23.2	94.9	61.5	6185	2066	2066	309	4.5	22.26	10
"	"	7. Diagonal Brace/Inner Cover Plate (AB)/Gusset	32.2	32.4	0	142843	1062	3097	386	4.5	17.78	10
SR-a	Yes	1. Outer Hood/Cover Plate (AB)	84.8	17	3.6	140575	318	2242	2104	6.22	3.26	10
"	"	2. Vertical Plate Inside Hood/Outer Hood (AB) <sup>(c)</sup>	84.8	25.6	54.5	142906	1419	2149	1812	6.49	3.79	10
"	"	3. Outer Top Cover/Vertical Plate Inside Hood (AB)	79.8	-25.6	61.5	140248	967	2025	1677	6.88	4.10	10

See Table 11.1a for notes (a) and (b).

Table 11.2a. Minimum stress ratios at zero frequency shift for the nodes listed in Table 11.1a computed using the EPU loads estimated from 2007 CLTP loads filtered with 2008 LP data and amplified with EPU bump-up factors.

Stress Ratio	Weld	Location	Location (in) <sup>(a)</sup>			node <sup>(b)</sup>	Stress Intensity (psi)			Stress Ratio	
			x	y	z		Pm	Pm+Pb	S <sub>alt</sub>	SR-P	SR-a
<b>SR-P</b>	<b>Yes</b>	<b>1. Lifting Rod Support</b>	<b>-50.6</b>	<b>77.8</b>	<b>0</b>	<b>152128</b>	<b>3353</b>	<b>3353</b>	<b>251</b>	<b>2.77</b>	<b>&gt;20</b>
"	"	2. Inner Top Cover/Rail	-11.1	95.4	61.5	141731	1332	3782	267	3.69	25.75
"	"	3. Middle Plate/Inner Cover Plate (AB)	1.8	0	0	143461	1225	3380	<250	4.12	>20
"	"	4. Inner Vane Bank (CD)	-1.8	-99.7	12	20042	2102	2102	<250	4.42	>20
"	"	5. Inner Cover Plate (CD)	-32.2	91.7	0	112814	602	3002	260	4.64	26.43
SR-a	Yes	1. Outer Hood/Outer Cover Plate (CD)	-84.8	-17	3.6	139060	337	2232	2226	6.25	3.09

See Table 11.1a for notes (a) and (b).

Table 11.2b. Minimum stress ratios at any frequency shift for the nodes listed in Table 11.1b computed using the EPU loads estimated from 2007 CLTP loads filtered with 2008 LP data and amplified with EPU bump-up factors.

Stress Ratio	Weld	Location	Location (in.) <sup>(a)</sup>			node <sup>(b)</sup>	Stress Intensity (psi)			Stress Ratio		% Freq. Shift
			x	y	z		Pm	Pm+Pb	S <sub>alt</sub>	SR-P	SR-a	
<b>SR-P</b>	<b>Yes</b>	<b>1. Lifting Rod Support</b>	<b>-50.6</b>	<b>77.8</b>	<b>0</b>	<b>152128</b>	<b>3552</b>	<b>3552</b>	<b>460</b>	<b>2.62</b>	<b>14.92</b>	<b>10</b>
"	"	2. Inner Top Cover/Rail	-11.1	95.4	61.5	141731	1389	3944	407	3.54	16.88	10
"	"	3. Middle Plate/Inner Cover Plate (AB)	1.8	0	0	143461	1294	3572	356	3.90	19.28	7.5
"	"	4. Inner Vane Bank (AB)	1.8	99.7	12	20737	2295	2295	499	4.05	13.78	10
"	"	5. Middle Vane Bank (AB)	23.2	94.9	12	11016	2285	2285	530	4.07	12.95	10
"	"	6. Top Vane Bank Bar	23.2	94.9	61.5	6185	2184	2184	422	4.26	16.27	10
"	"	7. Diagonal Brace/Inner Cover Plate (AB)/Gusset	32.2	32.4	0	142843	1111	3255	549	4.28	12.52	10
SR-a	Yes	1. Outer Hood/Cover Plate (AB)	84.8	17	3.6	140575	401	2992	2818	4.66	2.44	10
"	"	2. Vertical Plate Inside Hood/Outer Hood (AB) <sup>(c)</sup>	84.8	25.6	54.5	142906	2167	3259	2839	4.28	2.42	10
"	"	3. Outer Top Cover/Vertical Plate Inside Hood (AB)	79.8	-25.6	61.5	140248	1218	2608	2252	5.35	3.05	10

See Table 11.1a for notes (a) and (b).

Table 11.3a. Minimum stress ratios at zero frequency shift for the nodes listed in Table 11.1a computed using the unfiltered 2007 CLTP loads (i.e., signal noise has not been removed).

Stress Ratio	Weld	Location	Location (in) <sup>(a)</sup>			node <sup>(b)</sup>	Stress Intensity (psi)			Stress Ratio	
			x	y	z		Pm	Pm+Pb	S <sub>alt</sub>	SR-P	SR-a
<b>SR-P</b>	<b>Yes</b>	<b>1. Lifting Rod Support</b>	<b>-50.6</b>	<b>77.8</b>	<b>0</b>	<b>152128</b>	<b>3315</b>	<b>3315</b>	<b>&lt;250</b>	<b>2.80</b>	<b>&gt;20</b>
"	"	2. Inner Top Cover/Rail	-11.1	95.4	61.5	141731	1316	3740	<250	3.73	>20
"	"	3. Middle Plate/Inner Cover Plate (AB)	1.8	0	0	143461	1219	3366	<250	4.14	>20
"	"	4. Inner Vane Bank (CD)	-1.8	-99.7	12	20042	2069	2069	<250	4.49	>20
"	"	5. Inner Cover Plate (CD)	-32.2	91.7	0	112814	595	2967	<250	4.70	>20
SR-a	Yes	1. Outer Hood/Outer Cover Plate (CD)	-84.8	-17	3.6	139060	285	1871	1824	7.45	3.77

See Table 11.1a for notes (a) and (b).

Table 11.3b. Minimum stress ratios at any frequency shift for the nodes listed in Table 11.1b computed using the unfiltered 2007 CLTP loads (i.e., signal noise has not been removed).

Stress Ratio	Weld	Location	Location (in.) <sup>(a)</sup>			node <sup>(b)</sup>	Stress Intensity (psi)			Stress Ratio		% Freq. Shift
			x	y	z		Pm	Pm+Pb	S <sub>alt</sub>	SR-P	SR-a	
<b>SR-P</b>	<b>Yes</b>	<b>1. Lifting Rod Support</b>	<b>-50.6</b>	<b>77.8</b>	<b>0</b>	<b>152128</b>	<b>3481</b>	<b>3481</b>	<b>382</b>	<b>2.67</b>	<b>18.00</b>	<b>10</b>
"	"	2. Inner Top Cover/Rail	-11.1	95.4	61.5	141731	1372	3895	362	3.58	18.97	10
"	"	3. Middle Plate/Inner Cover Plate (AB)	1.8	0	0	143461	1271	3507	303	3.98	22.68	7.5
"	"	4. Inner Vane Bank (AB)	1.8	99.7	12	20737	2253	2253	449	4.13	15.31	10
"	"	5. Middle Vane Bank (AB)	23.2	94.9	12	11016	2167	2167	449	4.29	15.29	10
"	"	6. Top Vane Bank Bar	23.2	94.9	61.5	6185	2118	2118	358	4.39	19.19	10
"	"	7. Diagonal Brace/Inner Cover Plate (AB)/Gusset	32.2	32.4	0	142843	1101	3213	503	4.34	13.66	10
SR-a	Yes	1. Outer Hood/Cover Plate (AB)	84.8	17	3.6	140575	338	2383	2237	5.85	3.07	10
"	"	2. Vertical Plate Inside Hood/Outer Hood (AB) <sup>(c)</sup>	84.8	25.6	54.5	142906	1733	2622	2213	5.32	3.10	10
"	"	3. Outer Top Cover/Vertical Plate Inside Hood (AB)	79.8	-25.6	61.5	140248	1032	2222	1837	6.27	3.74	10

See Table 11.1a for notes (a) and (b).

Table 11.4a. Minimum stress ratios at zero frequency shift for the nodes listed in Table 11.1a computed using the EPU loads estimated from unfiltered 2007 CLTP loads (i.e., signal noise has not been removed).

Stress Ratio	Weld	Location	Location (in) <sup>(a)</sup>			node <sup>(b)</sup>	Stress Intensity (psi)			Stress Ratio	
			x	y	z		Pm	Pm+Pb	S <sub>alt</sub>	SR-P	SR-a
<b>SR-P</b>	<b>Yes</b>	<b>1. Lifting Rod Support</b>	<b>-50.6</b>	<b>77.8</b>	<b>0</b>	<b>152128</b>	<b>3383</b>	<b>3383</b>	<b>280</b>	<b>2.75</b>	<b>24.54</b>
"	"	2. Inner Top Cover/Rail	-11.1	95.4	61.5	141731	1349	3832	318	3.64	21.58
"	"	3. Middle Plate/Inner Cover Plate (AB)	1.8	0	0	143461	1237	3414	221	4.08	31.10
"	"	4. Inner Vane Bank (CD)	-1.8	-99.7	12	20042	2128	2128	253	4.37	27.17
"	"	5. Inner Cover Plate (CD)	-32.2	91.7	0	112814	615	3079	339	4.53	20.27
SR-a	Yes	1. Outer Hood/Outer Cover Plate (CD)	-84.8	-17	3.6	139060	352	2453	2407	5.68	2.85

See Table 11.1a for notes (a) and (b).

Table 11.4b. Minimum stress ratios at any frequency shift for the nodes listed in Table 11.1b computed using the EPU loads estimated from unfiltered 2007 CLTP loads (i.e., signal noise has not been removed).

Stress Ratio	Weld	Location	Location (in.) <sup>(a)</sup>			node <sup>(b)</sup>	Stress Intensity (psi)			Stress Ratio		% Freq. Shift
			x	y	z		P <sub>m</sub>	P <sub>m</sub> +P <sub>b</sub>	S <sub>alt</sub>	SR-P	SR-a	
SR-P	Yes	1. Lifting Rod Support	- 50.6	77.8	0	152128	3601	3601	504	2.58	13.62	10
"	"	2. Inner Top Cover/Rail	- 11.1	95.4	61.5	141731	1415	4018	478	3.47	14.37	10
"	"	3. Middle Plate/Inner Cover Plate (AB)	1.8	0	0	143461	1305	3603	400	3.87	17.15	7.5
"	"	4. Inner Vane Bank (AB)	1.8	99.7	12	20737	2389	2389	592	3.89	11.60	10
"	"	5. Middle Vane Bank (AB)	23.2	94.9	12	11016	2306	2306	593	4.03	11.58	10
"	"	6. Top Vane Bank Bar	23.2	94.9	61.5	6185	2240	2240	472	4.15	14.55	10
"	"	7. Diagonal Brace/Inner Cover Plate (AB)/Gusset	32.2	32.4	0	142843	1151	3374	664	4.13	10.34	10
<b>SR-a</b>	<b>Yes</b>	<b>1. Outer Hood/Cover Plate (AB)</b>	<b>84.8</b>	<b>17</b>	<b>3.6</b>	<b>140575</b>	<b>423</b>	<b>3131</b>	<b>2953</b>	<b>4.45</b>	<b>2.33</b>	<b>10</b>
"	"	2. Vertical Plate Inside Hood/Outer Hood (AB) <sup>(c)</sup>	84.8	25.6	54.5	142906	2231	3355	2921	4.16	2.35	10
"	"	3. Outer Top Cover/Vertical Plate Inside Hood (AB)	79.8	- 25.6	61.5	140248	1290	2825	2424	4.94	2.83	10

See Table 11.1a for notes (a) and (b).

Table 11.5. Limiting alternating stress ratios at welds at CLTP and EPU conditions, with and without noise filtering, obtained by considering all nodes on a weld having an alternating stress ratio, SR-a<5 for noise-filtered CLTP loads.

Load Condition	Noise Filtered?	Limiting SR-a Locations	Location (in.) <sup>(a)</sup>			node <sup>(b)</sup>	Stress Intensity (psi)			Stress Ratio		% Freq. Shift
			x	y	z		Pm	Pm+Pb	S <sub>alt</sub>	SR-P	SR-a	
CLTP	Yes	Vertical Plate Inside Hood/Outer Hood AB <sup>(c)</sup>	84.8	25.6	54.5	142906	1669	2528	2132	5.52	3.22	10
"	"	Outer Hood AB/Outer Cover Plate AB	84.8	17.0	3.6	140575	318	2242	2104	6.22	3.26	10
"	"	Outer Top Cover AB/Vertical Plate Inside Hood	79.8	-25.6	61.5	140248	967	2025	1677	6.88	4.10	10
CLTP	No	Outer Hood CD/Outer Cover Plate CD	-84.8	-17.0	3.6	139060	332	2282	2250	6.11	3.05	-10
"	"	Vertical Plate Inside Hood/Outer Hood AB <sup>(c)</sup>	84.8	25.6	54.5	142906	1733	2622	2213	5.32	3.10	10
"	"	Outer Top Cover AB/Vertical Plate Inside Hood	79.8	-25.6	61.5	140248	1032	2222	1837	6.27	3.74	10
EPU	Yes	Vertical Plate Inside Hood/Outer Hood AB <sup>(c)</sup>	84.8	25.6	54.5	142906	2167	3259	2839	4.28	2.42	10
"	"	Outer Hood AB/Outer Cover Plate AB	84.8	17.0	3.6	140575	401	2992	2818	4.66	2.44	10
"	"	Outer Top Cover AB/Vertical Plate Inside Hood	79.8	-25.6	61.5	140248	1218	2608	2252	5.35	3.05	10
EPU	No	Outer Hood CD/Outer Cover Plate CD	-84.8	-17.0	3.6	139060	415	2998	2971	4.65	2.31	-10
"	"	Vertical Plate Inside Hood/Outer Hood AB <sup>(c)</sup>	84.8	25.6	54.5	142906	2231	3355	2921	4.16	2.35	10
"	"	Outer Top Cover AB/Vertical Plate Inside Hood	79.8	-25.6	61.5	140248	1290	2825	2424	4.94	2.83	10

No stress reduction factors (SRFs) have been applied to these results.

For sets of nodes that are exact mirror images of each other (i.e., the location corresponds to another node reflected across x=0 and/or y=0) only the limiting location is reported.



See Table 11.1a for notes (a) and (b).

(c) This location has an SRF=0.85. However, it has not been applied in the tabulated results presented here.

EMCB-SD RAI No. 12

NSPM states on page 33 of CDI Report 07-26P that the bias error associated with finite mesh discretization, [[

(3)]]

NSPM Response

[[

(3)]]

EMCB-SD RAI No. 13

It is unclear which high stress location(s) in the steam dryer full FE model based on shell elements are further investigated using solid element sub-models in SIA calculation package 0801040.301. Location 2 in Figure 14d in CDI Report 07-26P is close to Location 2 in the SIA package. Location 1 is sub-modeled by SIA, but the low stress reduction factor (0.97) is apparently not used by NSPM. Identify how many high stress regions in CDI Report 07-26P are adjusted using stress reduction factor determined from sub-modeling.

NSPM Response

There are four high stress regions in C.D.I. Report No. 07-26P that are adjusted using a stress reduction factor determined from sub-modeling. A further discussion follows.

The 0.97 stress reduction factor (SRF) was not used because it was close to unity and was not needed in the C.D.I. Report No. 07-26P (Rev. 2) submission. The smaller SRF of 0.39 (now revised to 0.85 per the response to RAI 16) was applied to only four nodes, which are mirror images of each other (i.e., one point reflected across the  $x = 0$  and/or  $y = 0$  planes). Because the results in C.D.I. Report No. 07-26P used  $SRF = 0.39$  for these locations, none of the points appeared in the table, since the resulting stress ratio

after application of the SRF was much higher than 5.0. The revised values using no SRF are presented in Table 11.5 at CLTP and EPU conditions.

#### EMCB-SD RAI 14

The body of Tables 6 to 9 of CDI Report 07-26P does not identify the applicability of Note c given with the tables. The licensee is requested to identify the specific data to which Note (c) applies.

#### NSPM Response

Note (c) is a general comment of clarification pertaining to the Tables to point out that the nominal stress intensities at the vertical plate/outer hood support junction are multiplied by the stress reduction factor (SRF) of 0.39 (now 0.85 per the response to RAI 16). The resulting stresses at these nodes are sufficiently low that the nodes do not show up in the Tables. For example, in Table 6a, one can infer that the nodes on this vertical plate/outer hood support junction have alternating stresses at zero shift below 910 psi, which is the smallest alternating stress intensity listed in that Table. The detailed results for those nodes where note (c) apply are given in the response to RAI 13.

#### EMCB-SD RAI No. 15

Provide a detailed Monticello steam dryer monitoring plan to be followed during the initial power ascension from CLTP to EPU power. The plan may include pre-defined hold points and plateaus allowing time for analysis and evaluation, monitoring of moisture carryover and steam dryer load signals, and long-term steam dryer inspections to verify the steam dryer performance. The plan should include acceptance criteria for continued power ascension and identify the actions to be taken when level 1 and level 2 limit curves are violated. The plan should also include licensing conditions.

#### NSPM Response

The power ascension test procedure will be based on NSPM procedure 8303 which governed the power re-rate power ascension testing performed in 1998 to increase power from 1670MWt to 1775 MWt. This procedure provides the overall management oversight and control of the activities requiring completion to assure MNGP can operate safely up to an interim power level of approximately 1865 MWt. This is the estimated maximum power level that is achievable based on installed equipment as of the end of the 2009 refueling outage. Equipment modification or replacement in the 2011 refueling outage will enable operation at full EPU power of 2004 MWt.

Power ascension testing starts with the reactor at CLTP of 1775 MWt. Reactor power is reduced to 90% CLTP or approximately 1598 MWt, the rod pattern is set to support power ascension and base line walkdowns and data are taken for various plant parameters including steam dryer performance. Steam dryer loading data is taken from the strain gages on the main steam piping and is analyzed as described in Section 5 of Enclosure 11 in the MNGP EPU License Amendment Request (L-MT-08-052). Moisture carryover performance is evaluated using existing plant procedure I.03.29. These data are also taken and analyzed at each of the additional power levels listed below. The analysis of strain gage data and moisture carryover is expected to require a minimum of 24 hours, resulting in a minimum 24 hour hold at each power level.

95% CLTP	1686 MWt
100% CLTP	1775 MWt
102.5% CLTP	1820 MWt
105% CLTP	1865 MWt

The steam dryer tests will include current industry standards for evaluation of steam dryer capability based on the use of limit curves and analysis. Power ascension testing is discussed in Section 5 of Enclosure 11 of the MNGP EPU LAR dated November 5, 2008. It is further discussed below. The stress ratio and limit curves provided in Enclosure 11 are superseded by this RAI response.

Note: The maximum power level of 105% CLTP may not be achievable due to other plant equipment limitations until completion of all modifications in 2011. Following completion of all modifications testing will continue using 2.5% step increases until full EPU power level of 2004 MWt is achieved.

Acceptance criteria are specified by two levels. Level 1 acceptance criteria for the steam dryer are defined by the limit curves. Level 1 criteria, as used in this context, have been established for steam dryer performance monitoring, these criteria are based on the maximum design allowable limit. If a Level 1 limit curve is not satisfied, the plant will be returned to a power level where the Level 1 limit curve is satisfied. The Level 1 criterion which was not satisfied SHALL be resolved, and steam dryer structural integrity evaluated, before power is increased. Following a Level 1 resolution, applicable tests may be repeated to verify the Level 1 criterion is satisfied. MNGP will provide the evaluation of steam dryer structural integrity to the NRC staff prior to further increases in reactor power when increasing to power levels above CLTP.

Level 2 criteria are defined by the limit curves. If a Level 2 limit curve is not satisfied, operating and testing plans would not necessarily be altered. Level 2 criteria as used for steam dryer monitoring are 80% of the Level 1 criterion.

When a Level 2 criterion is not satisfied, an investigation of the measurements and the analytical prediction techniques will be completed prior to any power level increase. Following an evaluation of the equipment Level 2 performance data versus the predictor and the design allowable value, the limit may be changed by the Responsible Cognizant Engineer.

EMCB-SD RAI No. 16

In Structural Integrity Associates Calculation Package 0801040.301, "Monticello Steam Dryer Sub-model Analysis", dated 10/31/2008, NSPM performs a sub-model analysis for the double-sided fillet weld between the outer hood and the gusset using solid elements. The results show that the shell-element full model over-predicts stress intensity at the weld and the corresponding stress intensity over-prediction factor is 2.56 (= 1/0.39). There appears to be some justification for such a high over-prediction factor because the location includes a double-sided fillet weld. However, there are two major concerns about this high over-prediction factor as discussed below:

- i. The stress intensity profile (both magnitude and distribution) at the fillet weld in the shell-element sub-model is significantly different than that in the full-shell model as shown in Table 5-1. The magnitude of the stress intensity in the sub-model is up to 7.1 times higher. NSPM should justify that the stress intensity over-prediction factor determined using such a significantly different stress profile would be applicable to the NSPM steam dryer stress analysis presented in CDI Report 08-15P, Rev. 2.
- ii. The sub-modeling approach presented in the SIA Calculation Package 0801040.301, "Monticello Steam Dryer Sub-model Analysis", 10/31/2008 is not a typical or standard conventional sub-modeling approach. In a typical sub-modeling approach, as employed in the general purpose finite element codes such as ANSYS and ABAQUS, the results from the full model analysis are mapped or interpolated onto the corresponding nodes within the appropriate part of the boundary (cut boundary) of the sub-model. These loads and any other loads simulating the pressure and inertia loading applied to the local region are used to perform the detailed finite element analysis of the sub-model from which the stress ratios may be determined. As NSPM's sub-modeling approach is not typical and different from the standard conventional sub-modeling approach, it is not certain that the corresponding result for the stress intensity over-prediction factor is conservative. Based on the observation noted in item (i) above, the staff is not endorsing this non-traditional sub-modeling approach, for use on a generic basis for EPU applications. The licensee is requested to validate this non-traditional sub-modeling approach or replace with a typical conventional sub-modeling analysis for the particular location of the steam dryer.

NSPM Response

Response to Part i of the RAI follows:

Structural Integrity Associates Calculation Package 0801040.301, "Monticello Steam Dryer Submodel Analysis," has been revised to address RAI 16. Two outer hood analyses have been performed, and they are described as follows:

1st Analysis - Scaling Down the Applied Load On Outer Hood

In this analysis, the applied loads on the outer hood analysis are scaled down so that the maximum applied nodal stress intensity in the Shell Submodel analysis matches the maximum nodal stress intensity in the CDI Shell model. This analysis is documented in Section 5.0 of Calculation 0801040.301, Rev. 1.

In scaling down the applied load, the stress intensity comparison between the CDI Shell model and the Shell Submodel is provided in Table 16.1:

Table 16.1 - Outer Hood Stress Profile Comparison

CDI Shell Model		Shell Submodel	
Node	Stress Intensity (psi)	Node	Stress Intensity (psi)
140301	4,303	20005	4,303
140300	952	67206	2,701
140307	642	67202	2,656
140306	530	67198	2,811

Table 16.1 shows that an exact match is obtained at CDI Shell Model Node 140301, which has the maximum nodal stress intensity. For the neighboring nodes, higher nodal stress intensities have been imposed on the Shell Submodel.

Based on the above scaled down applied loads, the computed solid model / shell model stress ratio is **0.85**.

In the course of performing the above analysis, an inadvertent book-keeping error was discovered in the spreadsheet that calculates the stress ratio for the outer hood analysis. Incorrect data were pasted into one of the worksheets that resulted in computing errant stress ratio documented in the Revision 0 of the calculation. This

spreadsheet has been revised, and the affected tables in the calculation have been updated to reflect the correct data and stress ratio.

2nd Analysis - Alternative Load Pattern On Outer Hood

The objective of this analysis is to obtain a better match of the stress intensity profile between the CDI Shell model and the Shell Submodel. This is accomplished by applying an alternative load pattern on the outer hood. The details of this analysis are provided in Appendix B of calculation 0801040.301, Rev. 1.

In applying an alternative load pattern, the stress intensity comparison between the CDI Shell model and the Shell Submodel is provided in the following table:

Table 16.2 - Alternative Load Pattern Outer Hood Stress Profile Comparison

CDI Shell Model		Shell Submodel	
Node	Stress Intensity (psi)	Node	Stress Intensity (psi)
140301	4,303	20005	4,303
140300	952	67206	2,279
140307	642	67202	1,697
140306	530	67198	1,240

With reference to the above Table 16.2, exact match is obtained at CDI Shell Model node 140301, which has the maximum nodal stress intensity. The nodal stress intensities imposed on the neighboring nodes in the Shell Submodel remain higher. However, the magnitude of difference is considerably lower than the differences associated with the 1st analysis, as documented in Table 16.1.

Based on the above alternative load pattern, the computed solid model / shell model stress ratio is **0.82**, a small reduction from the stress ratio of 0.85 computed in the 1st analysis above.

## Conclusion

Both the 1st and 2nd analyses compute stress ratios that are comparable to each other. Note that the stress intensity profile in the 2nd analysis is a better match to the CDI Shell model stress intensity profile, but, is less conservative than the 1st analysis. Correspondingly, the computed stress ratio is lower at 0.82. Therefore, the use of a stress ratio of 0.85 is considered to be reasonable, and conservative, and will henceforth be used instead of 0.39.

Response to Part ii of the RAI follows:

A separate Structural Integrity Associates calculation 0900474.301, "Comparison Study of Substructure and Submodel Analysis using ANSYS," has been prepared to address the concern over the use of the sub-modeling approach. The following is a summary of the approaches and the key findings and conclusions documented in the calculation.

## Nomenclature

Submodel: This refers to a subpart of the full model that has been developed for use in either the substructure analysis or the submodel analyses. There are two submodels used in this comparison study: submodel #1 and submodel #2. The submodel #1 is 1/2 the size of the full model, and submodel #2 is 3/4 the size of the full model.

Substructure Analysis: Substructure analysis refers to a typical analysis approach, as employed in the general purpose finite element codes such as ANSYS. In this approach, the displacements from the full model analysis are interpolated and mapped onto the nodes on the appropriate submodel boundaries. These nodal displacements along the boundaries and any loads applied to the local region determine the solution of the submodel.

Submodel Analysis: In a submodel analysis, two submodels are created: one is based on shell elements and the other solid elements. The shell submodel is used to match the stress profile in the submodel with the corresponding stress profile of the full shell model. This matching of stress profile is an iterative process. This is performed by applying loads or displacements, typically along a line. When a close match of the stress profile is achieved, the established loads or displacements can then be applied to the corresponding solid submodel stress analysis. Appropriate boundary conditions are required to be applied to the submodel boundaries. A stress reduction factor (SRF) is calculated by comparing the solid submodel result to the corresponding full shell model result. The SRF is then applied to the appropriate stresses in the full model shell analysis.



**Stress Reduction Factor (SRF):** This refers to the ratio of the maximum solid submodel linearized stress intensity and the maximum full shell model stress intensity, at the location of interest. Mathematically, SRF is defined as "Solid Submodel Maximum Linearized  $P_m + P_b$  Stress Intensity (along solid submodel stress paths) / Full Shell Model Maximum  $P_m + P_b$  Stress Intensity".

### **Approach and Scope**

In this comparison study, the analyses are performed using a structure consisting of two plates: a horizontal plate (6" wide by 20" long by 1/4" thick) welded along the 6" edge to a vertical plate (10" wide by 40" tall by 1/2" thick) centrally at mid height location using 1/4" double-sided fillet weld. It is also assumed that the fillet weld is provided at both ends of the horizontal plate, with rounded transition from the end fillet weld to the side fillet weld. The top and bottom edges of the vertical plate are fixed. This configuration is subjected to finite element modeling and analysis using full shell, full solid, shell submodel and solid submodel techniques to determine comparative SRFs. Additional details for all models are provided in Section 3.1 of SI Calculation No. 0900474.301.

The load cases include:

1. Load Case #1: Apply a load that generates primarily bending stress through the thickness of the horizontal plate.
2. Load Case #2: Apply a load that generates primarily membrane stress in the horizontal plate.

The analysis cases include:

1. Static analysis by applying a static uniform load at the free edge of the horizontal plate.
2. Dynamic time history analysis by applying a harmonic uniform load at the free edge of the horizontal plate.

The computed SRFs include:

1. Full Solid Model Analyses: The full solid model is the same size as the full shell model except that it is generated using solid elements and includes detailed modeling of the welds. SRF for a load/analysis case is the ratio of the maximum linearized membrane plus bending stress at the weld from the full solid model to the maximum stress from the full shell model for the same load/analysis case. These SRFs provide a baseline against which the accuracy and conservatism of both the substructure and submodel techniques may be judged.

2. Substructure Analyses: The substructure analyses apply boundary displacements along the perimeter of substructure models generated with shell elements. The boundary displacements are extracted from the full shell model analysis results along the lines that coincide with the substructure model boundaries. The same displacements are then applied to substructure models generated using solid elements and including detailed modeling of the welds. SRF for each load and analysis case is the ratio of the maximum linearized membrane plus bending stress from the solid substructure model to the maximum stress in the joint from the full shell model.
3. Submodel Analyses: The submodel analyses apply displacements or loads to a submodel generated using shell elements to match stress intensity along the weld line common to both the full shell and submodel. These loads or displacements are then applied to a submodel of the same size as the shell submodel but generated using solid elements and including detailed modeling of the weld. SRF for a load/analysis case is the ratio of the maximum linearized membrane plus bending stress at the weld from the solid submodel to the maximum stress from the full shell model.

**Key SRF Comparison**

**Static Analysis SRF Comparison**

Load Case #1	SRF	Load Case #2	SRF
Full Solid Model Baseline Analysis	0.59	Full Solid Model Baseline Analysis	0.89
Substructure Analysis <sup>(1)</sup>	0.69	Substructure Analysis <sup>(1)</sup>	0.91
Submodel Analysis <sup>(1)</sup>	0.66	Submodel Analysis <sup>(1)</sup>	0.89

Note: (1) SRF is computed using submodel #2. The SRF computed using submodel #1 is provided in the calculation, but, has been excluded in this executive summary for brevity.

**Dynamic Analysis SRF Comparison**

Load Case #1	SRF	Load Case #2	SRF
Full Solid Model Baseline Time History Analysis	0.59	Full Solid Model Baseline Time History Analysis	0.89
Substructure Time History Analysis <sup>(1)</sup>	0.68	Substructure Time History Analysis <sup>(1)</sup>	0.91
Submodel (Static) Analysis <sup>(1)</sup>	0.66	Submodel (Static) Analysis <sup>(1)</sup>	0.89

Note: (1) SRF is computed using submodel #2.

The solid model baseline analysis does not include any inherent approximation or assumption that is associated with the substructure and submodel analyses. The SRFs computed using the solid model baseline analysis provides accurate benchmarks for comparison.

The comparison of the SRF provided in the above tables show that:

- The SRFs computed using the full solid to full shell model comparison confirm that shell model stress results are conservative for configurations which represent the double fillet welds used in many MNGP Steam Dryer plate-to-plate joints. This is indicated by the computed SRFs of 0.59 and 0.89 for Load Cases 1 and 2, respectively (i.e., both < 1.0). Furthermore, these SRFs were found to be invariant for both static and dynamic analyses.
- The SRFs computed using the substructure analysis are generally higher than the SRFs computed using the solid model baseline analysis. The SRFs are higher because in a substructure analysis the displacements from a more flexible shell model are applied onto the boundaries of a more rigid solid model, which includes the detailed weld configuration. This stiffness discrepancy between the shell and the solid models causes higher stresses to be computed in the solid model, thus resulting in higher SRF for the substructure analysis.
- The SRFs computed using the submodel analysis technique either match (Load Case 2) or provide a conservative bias (12% - Load Case 1) when compared to full model SRFs. Furthermore, these SRFs are invariant for static and dynamic analyses.

### Conclusion

In conclusion, the comparisons above show that the SRFs computed using the submodel analysis approach are accurate and acceptable, and therefore, validate the submodel analysis approach used in the steam dryer stress analysis. The SRF of 0.39 is no longer used; instead a SRF of 0.85 is used.

### EMCB-SD RAI No. 17

NSPM has shown that the calculated alternating stresses near the cracks in the MNGP dryer (based on ACM loads applied to a finite element model) are much lower than the fatigue stress limit of 13,600 psi. This indicates that acoustic pressures that are measurable in the MSLs are not responsible for the appearance of the cracks or the stress analysis results presented in CDI Report 07-26P are non-conservative and inaccurate.

- i. The licensee is requested to provide rationale for why the stress analysis results are not consistent with its operating experience.
- ii. Explain what phenomena cause these cracks.
- iii. Discuss how those phenomena might change at EPU conditions.
- iv. Explain whether cracks like these appeared in other BWR/3 square hood dryers at CLTP conditions?
- v. Provide any experience information gained thus far pertaining to these cracks and their growth from the plants that have been operating at EPU conditions?

### NSPM Response

Reference [1] addressed cracking in three components: end plate, guide channel, and drain channel. Each component will be addressed separately, below.

#### **Steam Dryer End Plate Cracking**

The questions contained in this RAI are largely addressed in [2]; excerpts from this reference are provided following this paragraph. Operation at EPU will have no effect on fabrication induced stresses or stress concentrations contributed by the fabrication process or weld configuration. Flow induced vibration (FIV) fluctuating stress amplitudes are expected to increase at EPU operating conditions; however, the FIV stress analysis provides a predictive assessment of these stresses and the power ascension monitoring program to be performed will acquire main steam line vibration data that will be used to develop operating loads as well as to identify whether any additional loads are introduced into the system during EPU operation.

*The weld V10 90 degrees was initially inspected during the 2005 RFO and required follow up inspection in 2007. The follow up weld inspection resulted in an identified indication which is approximately 0.25" long on the opposite side the plate from the previously identified flaw. This indication is similar to other indications identified during the 2005 RFO. All three indications are non-branched and fully contained within the weld, suggesting a fatigue type crack.*

*Review of video data from the 2005 outage concluded that the area identified in 2007 was not inspected. It is concluded that inspectors did not inspect the area due to the discontinuity in weld (weld is not continuous across the top of V10 at 90 degrees) and concluded there was no more flaw to evaluate and commenced the characterization of the initially identified flaw.*

*These indications are consistent with recent field experience found at a BWR with a similar square hood steam dryer design as well as previous steam dryer field occurrences. The inspection of another square hood steam dryer found two*

*cracks diametrically opposite to each other on the vertical weld located directly behind the lifting lug. The fabrication records for this other steam dryer indicated that high residual stresses developed during the welding sequence. Other “cold spring” type loading could have also been generated during fabrication. The high residual stresses, which act as a high mean stress, would tend to promote ... fatigue crack initiation under cyclic loading conditions ..*

*The indications on the Monticello steam dryer are similar (e.g., length and location) to the other steam dryer that had cracks at the top of the vertical weld behind the lifting rods and were fabricated by the same manufacturer. Thus, the Monticello steam dryer indications at Welds V3 90° (previously identified in 2005), V10 90°, and V10 270° (previously identified in 2005) were probably also fabricated using the same welding sequence resulting in elevated residual stresses. After the crack initiated, the residual stress would be reduced as the crack extended and the crack growth would slow, limiting the length of the flaw.*

*The indication is not expected to continue growing. Review of the previously identified indications at V3 90°, V10 90°, and V10 270° were re-inspected during the 2007 RFO. The re-inspection of the previously identified flaws did not identify any significant crack growth. The inspection substantiates the cause of the cracking was high residual weld stress left from fabrication. The newly identified indication at V10 90°, as discussed previously, was not inspected in 2005 as a result of obstruction or target fixation with the identified flaw.*

The indications at V3 90°, V10 90°, and V10 270° were re-inspected during the 2009 RFO. The re-inspection of the previously identified flaws did not identify any observable crack growth [5].

### **Steam Dryer Guide Channel Cracking**

The cracking observed in the steam dryer guide channel [3, 4] is atypical in that it is oriented perpendicular to the weld and proceeds from what appears to be an arc strike to the weld material joining the guide channel to the skirt. The indication appears to arrest at the weld material. A local stress concentration and material damage associated with the arc strike is the postulated initiation mechanism for this flaw. Field observations, from three successive inspections [3, 4], suggest this indication has arrested. If high cycle fatigue was a significant initiation and propagation mechanism for this flaw then the indication would have exhibited significant growth during the operating cycles between the 2005 and 2009 inspections. Although the FIV loading is expected to increase somewhat for EPU operation, the increase in FIV loading is not considered to be a factor affecting the behavior of this indication. NSPM is not aware of other examples of similar cracking; however, the postulated initiation mechanism is unrelated to operating power level and the atypical nature of this indication does not warrant special attention or concern for operation at EPU.

## **Steam Dryer Drain Channel Cracking**

The characteristics of the drain channel cover plate cracking are consistent with intergranular stress corrosion cracking (IGSCC) in that:

1. The indication is irregular and exhibits branching along its length.
2. The indication occurs in and remains within the heat affected zone (HAZ) of the material. The HAZ in stainless steel is a well known sensitization region.
3. The region exhibits multiple initiation sites in the HAZ around the perimeter of the cover plate.

High cycle fatigue is not considered to be an initiation mechanism for these indications; thus, low FIV stresses in this region are consistent with the observed crack characteristics. FIV stresses are expected to increase somewhat for EPU operation; however, they will not affect the nature of IGSCC initiation in sensitized materials. IGSCC is a common degradation mechanism in sensitized BWR materials and is commonly observed in various dryer components. The drain channel indications were re-inspected during the 2009 RFO. The re-inspection of the previously identified flaws did not identify any observable crack growth [5].

### References:

1. "Flaw Evaluation and Vibration Assessment of Existing Monticello Steam Dryer Flaws for Extended Power Uprate," SI Report No. 0800760.401, Revision 1, December 2008.
2. Engineering Evaluation 10451 contained in Design Information Transmittal EPU-0284.
3. Monticello RF0-22 Steam Dryer In-Vessel Visual Inspection Final Report, AREVA 2005.
4. Monticello RF0-23 Steam Dryer In-Vessel Visual Inspection Final Report, AREVA 2007.
5. Monticello RF0-24, In-Vessel Visual Examination Final Report, AREVA 2009.

### EMCB-SD RAI No. 18

Structural Integrity Analysis Report 0800760.401, Rev. 1 recommends that visual inspections of the NSPM dryer be conducted at all future refueling outages to monitor

the cracks that currently exist in the dryer. NSPM is requested to formally commit to such visual inspections as a condition for its EPU license.

### NSPM Response

MNGP inspection and evaluation guidelines have been developed based on the BWRVIP guidelines. The MNGP BWRVIP Inspection Plan identifies inspections of the known indications in the steam dryer as follows:

#### 2007 outage

Repeat Inspection of Indications Discovered During 2005 RFO. Per BWRVIP MEMO 2007- 362 (RAI No. 139-9) reinspection of unrepaired flaws shall be reperformed until it is demonstrated flaws have stabilized.

#### 2009 outage

Repeat Inspection of Indications Discovered During 2005 RFO and 2007 RFO. Per BWRVIP MEMO 2007- 362 (RAI No. 139-9) reinspection of unrepaired flaws shall be reperformed until it is demonstrated flaws have stabilized.

#### 2011 outage

Perform a new baseline inspection per BWRVIP MEMO2007-362 (RAI 139-9) which requires that a repeat of baseline inspections be performed in the next scheduled outage following an increase in power more than 2% above current licensed thermal power.

Subsequent outage steam dryer inspections will continue based on the guidance of BWRVIP MEMO 2007-362.

### EMCB-SD RAI No. 19

Structural Integrity Analysis Report 0800760.401, Rev. 1 asserts that the cracks reported in the steam dryer will have a negligible effect on the dryer stiffness because their sizes are small. Therefore, the dryer FE model does not need to be updated to include the cracks. However, the small cracks, depending on their locations, could impact the stiffness of the dryer and may influence the natural frequencies and mode shapes. The staff, therefore, requests NSPM to provide a detailed justification that these cracks have a negligible effect on the dryer natural frequencies, mode shapes and, therefore, on the stresses.

### NSPM Response

The cracking observed in the Monticello steam dryer will not affect the vibration response of the steam dryer sufficiently such that the finite element model (FEM) created for the EPU stress analysis does not need to be modified to incorporate cracking.

To justify that the cracks do not affect the FEM used in the FIV stress analysis, finite element analyses were performed [1] to simulate the cracked components and show that the modal responses, for the frequency range of interest, are not affected. Separate analyses were performed to assess the effects of cracks for the end plates, guide channel, and drain channel.

### Steam Dryer End Plates

The methodology used to address this RAI is:

1. Perform a modal analysis of the subject component (plate, drain channel, etc.) in the uncracked condition and extract all modes in the frequency band  $0 < f < 250$  Hz. The frequency band chosen is consistent with the frequency band generally monitored for FIV of steam dryers.
2. Perform a modal analysis of the subject component in the cracked condition and extract all modes in the same frequency band.
3. Compare natural frequencies and mode shapes in order to assess the “effect” of cracking on the component.
4. If the effect of cracking is shown to be small, in the evaluations performed, for the steam dryer component, then it is reasonable not to re-run a full stress analysis of the “cracked” Monticello steam dryer. Further, if the effect of cracking is small, then this effect can be considered to contribute an “error” term for the



modal solution of the dryer that is bounded by the current frequency shift incorporated into the CDI stress analysis and the effect of cracking can be said to already be incorporated in the existing analysis process.

The results of the end plate modal analysis show that no modes exist in the frequency band of relevance ( $0 < f < 250$  Hz) for steam dryer acoustic loading for both the cracked and uncracked configurations; thus, no actions are necessary to incorporate the effects of end plate cracking in the existing full dryer FEM.

### Steam Dryer Guide Channel

The cracking in the guide channel is very small and limited to a local region of the guide channel; further, the cracking does not create “flaps” or other local regions with significant reduction in constraint that would be expected to introduce local modes not present in the uncracked condition. The conservative method used to determine an upper bound of the effect of the guide channel cracking on the dynamic characteristics of the guide channel is outlined below:

1. Conservatively assume the crack reduces the area moment of inertia of the guide channel along its entire length rather than local to the cracked section only.
2. Calculate the area moment of inertia of the uncracked cross-section and the cracked cross-section. Standard statics principles are used to calculate the area moments of inertia for cracked and uncracked geometries.
3. Evaluate the bounding reduction in natural frequency of the guide channel using a handbook solution for transverse vibrations in beams.

Calculations were performed to determine the neutral axis of the channel and the area moment of inertia calculations for the cracked and uncracked guide channel configurations. The results of this calculation show that the effect of the observed guide channel cracking is found to be less than 10%.

The observed guide channel cracking does not have a significant effect on the dynamic characteristics of the steam dryer and does not require modification to the existing uncracked steam dryer FEM.

### Steam Dryer Drain Channel

The overall methodology used to address this component is described below.

1. Perform a modal analysis of the subject component (plate, drain channel, etc.) in the uncracked condition and extract all modes in the frequency band  $0 < f < 250$

Hz. The frequency band chosen is consistent with the frequency band generally monitored for flow induced vibration loading on steam dryers.

2. Perform a modal analysis of the subject component in the cracked condition and extract all modes in the same frequency band.
3. Compare natural frequencies and mode shapes in order to assess the “effect” of cracking on the component.
4. If the effect of cracking is shown to be small, in the evaluations performed, for the steam dryer component, then it is reasonable not to re-run a full stress analysis of the “cracked” Monticello steam dryer. Further, if the effect of cracking is small, then this effect can be considered to contribute an “error” term for the modal solution of the dryer that is bounded by the current frequency shift incorporated into the CDI stress analysis and the effect of cracking can be said to already be incorporated in the existing analysis process.

The conservative method used to assess the bounding effect of drain channel access hole cover plate cracking on the vibration characteristics of the steam dryer shows that the natural frequencies in the frequency band affected by steam dome FIV are reduced by less than 5%. This assessment assumed the entire cover plate was separated from the drain channel. The frequency shift already performed as a integral part of the steam dryer FIV stress analysis bounds the maximum effect of the access hole cover plate cracking; therefore, the observed drain channel cracking does not require modification to the existing uncracked steam dryer FEM.

Reference:

1. SI Calculation No. 0900474.303, Revision 1, “Response to NRC Request for Additional Information (RAI) EMCB-SD-RAI 17 and 19.”

EMCB-SD RAI No. 20

In the steam dryer evaluation for MNGP, the main steam line (MSL) strain gage measurements from 2007 at CLTP power level were reduced by subtracting 2008 data acquired at low power (LP) conditions in the plant.

According to Attachment II of Enclosure 11 to its letter of November 5, 2008, the licensee utilizes the acoustic circuit model (ACM), Rev. 4 (described in Reference 3, CDI Report 07-09P, Rev. 0) that was benchmarked using Quad Cities 2 (QC2) main steam line and steam dryer measurements. The licensee used the QC2 benchmark data to compute the frequency dependent bias errors and uncertainties for applying to MNGP. The MSL strain gage measurements used for the QC2 benchmark did not subtract LP data, whereas MNGP data used for dryer qualification subtracted the LP data.

[[

(3)]]

NSPM Response

[[

(3)]]